HHS Public Access

Author manuscript

Materialia (Oxf). Author manuscript; available in PMC 2022 March 01.

Published in final edited form as:

Materialia (Oxf). 2021 March ; 15: . doi:10.1016/j.mtla.2020.100954.

In-situ stable injectable collagen-based hydrogels for cell and growth factor delivery

Seyedsina Moeinzadeh[1], **Youngbum Park**[1,2], **Sien Lin**[1], **Yunzhi Peter Yang**[1,3,4,*]

[1]Department of Orthopedic Surgery, Stanford University, 300 Pasteur Drive, Stanford, CA 94305, USA

[2]Department of Prosthodontics, Yonsei University College of Dentistry, Seoul 120-752, Korea

[3]Department of Materials Science and Engineering, Stanford University, 496 Lomita Mall, Stanford, CA94305, USA

[4]Department of Bioengineering, Stanford University, 443 Via Ortega, Stanford, CA94305, USA

Abstract

Here we report development of in-situ stable injectable hydrogels for delivery of cells and growth factors based on two precursors, alginate, and collagen/calcium sulfate ($CaSO_4$). The alg/col hydrogels were shear-thinning, injectable through commercially available needles and stable right after injection. Rheological measurements revealed that pre-crosslinked alg/col hydrogels fully crosslinked at 37°C and that the storage modulus of alg/col hydrogels increased with increasing the collagen content or the concentration of $CaSO_4$. The viscoelastic characteristics and injectability of the alg/col hydrogels were not significantly impacted by the storage of precursor solutions for 28 days. An osteoinductive bone morphogenic protein-2 (BMP-2) loaded into alg/col hydrogels was released in 14 days. Human mesenchymal stem cells (hMSCs) encapsulated in alg/col hydrogels had over 90% viability over 7 days after injection. The DNA content of hMSC-laden alg/col hydrogels increased by 6–37 folds for 28 days, depending on the initial cell density. In addition, hMSCs encapsulated in alg/col hydrogels and incubated in osteogenic medium were osteogenically differentiated and formed a mineralized matrix. Finally, a BMP-2 loaded alg/col hydrogel was used to heal a critical size calvarial bone defect in rats after 8 weeks of injection. The alg/col hydrogel holds great promise in tissue engineering and bioprinting applications.

Graphical Abstract

[*]Corresponding author: Yunzhi Peter Yang, Ph.D., Department of Orthopedic Surgery, School of Medicine, Stanford University, 240 Pasteur Drive, BMI 258, Stanford, CA 94305, Tel: 650-723-0772, Fax: 650-724-5401, ypyang@stanford.edu.

Declaration of Competing Interest

The authors declare that they have no known competing financial interests or personal relationships that could have appeared to influence the work reported in this paper.

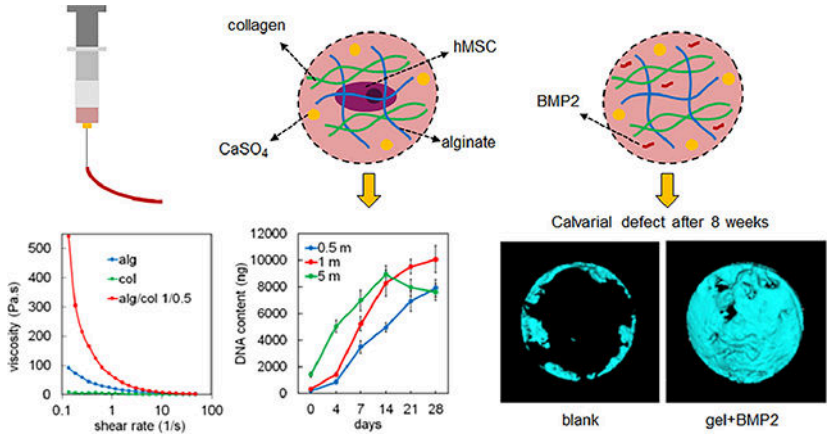

Keywords

injectable hydrogel; collagen; therapeutic delivery; human MSC; BMP2 protein; bone defect

1. Introduction

Injectable hydrogels have been extensively used as carriers for therapeutic delivery, including cells and proteins to the defect site in regenerative medicine [1–3]. Due to their large water content, porous microstructure and permeability to oxygen, nutrients, proteins and cell waste products, hydrogels provide an ideal three-dimensional (3D) microenvironment for cell encapsulation [4]. In addition, bioactive molecules can be incorporated into injectable hydrogels to promote cell adhesion, proliferation and differentiation of stem cells [5].

In-situ crosslinkable injectable hydrogels that are liquid before injection, are influenced by the in-vivo microenvironment prior to crosslinking, may leak from the defect site into the neighboring tissues, and dilute with the body fluid before gelation [6, 7], or need additional stimuli such as light or heat for crosslinking. Shear-thinning injectable hydrogels, that are partially or fully crosslinked before injection, flow through syringe and needles under the applied shear stress and take the shape of the defect cavity. These pre-crosslinked shear-thinning hydrogels are relatively stable and don’t leak out, get diluted or washed away after injection [6, 8]. Further, due to a protective effect of hydrogel, cells delivered in pre-crosslinked shear-thinning hydrogels have higher viability following injection compared to the cells delivered in solutions [8–10]. Therefore, shear-thinning hydrogels have recently been used not only as carriers for delivery of cells and therapeutics to the regeneration site, but also as bioinks for 3D bioprinting of tissues [11–14].

Alginate hydrogels are biocompatible and non-immunogenic hence good candidates for cell and therapeutics delivery [15]. A typical method for making alginate gel is instantaneous crosslinking of alginate in the solutions of water-soluble salts of divalent cations (e.g. $CaCl_2$) [16]. The strong local crosslinks and inhomogeneity in the crosslink density of the alginate hydrogels prepared via this instantaneous gelation method hinder the injectability and printability of the hydrogel [10, 17]. Alginate hydrogels with improved crosslinking

distribution and injectability have been made using divalent cation salts of low solubility including $CaSO_4$ [10, 18, 19]. Although injectable alginate hydrogels are biocompatible, they lack adhesive ligands that are required for cell survival, growth and proliferation within a 3D matrix. Modification of alginate molecule with cell adhesive peptides have been used to impart cell-adhesive ligands to alginate hydrogels [20–22] but short peptides lack the full function and specificity of native extracellular matrix (ECM) proteins [23, 24].

Collagen is the most abundant protein component of the ECM that contribute to the structure and function of tissues [25]. Collagen directly interacts with multiple integrin receptors on the cell surface including α1β1, α2β1, α11β1, and αVβ3 integrins, as well as the discoidin domain receptor tyrosine kinases 1 and 2 (DDR1 and DDR2) [26, 27]. In addition, collagen is indirectly sensed by cells through interaction with cell-binding proteins [27]. The cell-collagen interaction has been shown to play a key role in regulation of cell adhesion, proliferation and differentiation [28]. For example, the survival and osteogenic differentiation of hMSCs in collagen type I depend on interactions between collagen and both α2β1 and α11β1 integrins [29]. Due to the unique properties of collagen, collagen-based hydrogels closely mimic the native tissue microenvironment and have been widely used as 3D scaffolds for cell encapsulation in tissue engineering applications [30, 31]. Crosslinked collagen hydrogel is not injectable whereas uncrosslinked collagen hydrogel precursor solution is an injectable liquid and has been used for delivery of cells in regenerative medicine [32, 33]. However, as mentioned above, cell delivery in liquid formulations suffers from potential dilution and leakage to neighboring tissues due to a lack of stability in the target site. Also, a low viscosity and inferior structural stability of collagen precursor solution, limits its application as bioink in 3D bioprinting [34]. A number of strategies such as mixing pre-assembled collagen fibrils with injectable alginate hydrogel, or exposing the alginate/collagen mixtures to Ca^{2+} solution have been tested to increase the stability of collagen-based hydrogel following injection and to tune the physicomechanical characteristics of hydrogel [35–40]. However, these methods need collagen fibrils preprocessing, uncrosslinked solution postprocessing, and/or using special instrumentation such as coaxial nozzles or luer-lock syringes. Here we reported a facile method to make injectable collagen/alginate/$CaSO_4$ hydrogels. The effect of alginate to collagen weight ratio and $CaSO_4$ content on shear-thinning properties, injectability, and storage modulus of the hydrogels were investigated. In addition, the hydrogels microstructure, distribution of alginate and collagen within the hydrogel, degradation rate, and release kinetics of a model protein (BSA) and an osteo-inductive protein (BMP2) from the hydrogels were studied. Further, the viability, proliferation, and osteogenic differentiation of hMSCs in hydrogels were evaluated. Finally, the effect of the BMP2-laden alg/col hydrogel on bone repair of a critical size calvarial bone defect model in rats was evaluated.

2. Materials and Methods

2.1. Materials

Rat tail collagen type I was purchased from Corning Inc. (Corning. NY, USA). Sodium alginate (alginate, 500GM) was purchased from Pfaltz & Bauer Inc. (Waterbury, CT, USA). Sodium hydroxide (NaOH), ethanol, 5-(Aminomethyl)Fluorescein Hydrochloride, and Texas

Red™-X, Succinimidyl Ester were purchased from Thermo Fisher Scientific (Waltham, MA). Calcium sulfate ($CaSO_4$), 2-(N-Morpholino)ethanesulfonic acid (MES), N-(3-Dimethylaminopropyl)-N-ethylcarbodiimide hydrochloride (EDC), N-Hydroxysulfosuccinimide (NHS), dexamethasone, ascorbic acid, β-sodium glycerophosphate, and Human BMP2 ELISA kit were received from Sigma-Aldrich (St Louis, MO). Collagenase, Calcein AM/Ethidium homodimer-1 Live/Dead assay kit, and Quant-iT PicoGreen DNA assay kit were purchased from Thermo Fisher Scientific (Waltham, MA). QuantiChrom alkaline phosphatase activity (ALP) kit and Calcium Assay kit were purchased from BioAssay Systems (Hayward, CA, USA). Human BMP2 protein was provided by Medtronic (Dublin, Ireland).

2.2. Methods

2.2.1. Hydrogel preparation—A schematic representation of the method used to prepare alg/col hydrogels is shown in Figure 1. Alginate was dissolved in calcium free DMEM medium at 1% (w/v) concentration. The solution was filtered using a 0.22 μm PES filter (Millex, Millipore Sigma) and supplemented with sterile 1N NaOH at 4, 8, or 16 μL/mL to prepare alginate precursor solution for alg/col 1/0.25, alg/col 1/0.5 or alg/col 1/1 hydrogels, respectively. The alginate precursor solution was sterilized by filtration using 0.22 μm Millex syringe filters and stored at 4°C. Calcium sulfate ($CaSO_4$) was sterilized using electron beam (E-beam) at a 25 kGy dose, following ISO 11137– 2:2006 standard as previously described [41]. DI water was sterilized using a 0.22 μm PES filter. 1 mL sterile DI water was then added to 100 mg sterile $CaSO_4$ and the suspension was vortexed for 5 minutes. 750, 500, or 0 μL calcium free DMEM medium was added to 250, 500 or 1000 μL of collagen stock solution (collagen I from rat tail, Corning Inc) at 4°C, for alg/col 1/0.25, alg/col 1/0.5 or alg/col 1/1 hydrogels, respectively. Then, the collagen solution was supplemented with 0, 10, 20, or 30 μL of vigorously vortexed $CaSO_4$ suspension (corresponding to 0, 0.5, 1, and 1.5 mg/mL $CaSO_4$ concentrations in the hydrogel) and mixed via pipetting to make collagen precursor solution. The collagen precursor solution was added to the alginate precursor solution at 1:1 volume ratio and pipetted multiple times. To make pure alginate hydrogel (alg), alginate was dissolved in calcium free DMEM medium at 1% (w/v) concentration. 20 μL of vigorously vortexed $CaSO_4$ suspension (100 mg/mL) was suspended in 1 mL of calcium free DMEM medium. Then alginate solution and $CaSO_4$ suspension were mixed at 1:1 ratio. To make pure collagen hydrogel (col), collagen stock solution was added to calcium free DMEM medium to make a 2.5 mg/mL collagen solution (corresponding to collagen concentration in alg/col 1/0.5 gel) and the pH was adjusted to 7.4 using sterile 1N NaOH.

2.2.2. Rheological measurements and injectability—The alg/col hydrogels with different alginate/collagen weight ratios or $CaSO_4$ concentrations, were prepared at 4°C and loaded on the Peltier plate of an ARES-G2 rheometer (TA Instruments, New Castle, DE). An 8 mm parallel plate stainless steel geometry was used at a gap distance of 200 μm. To test the shear thinning characteristics, the viscosity of the hydrogels at 4°C was measured when the shear rate increased from 0.1 to 50 Hz. To test the temperature-responsive evolution of the storage modulus of the gels, the gels were equilibrated at 4°C for 15 minutes on the Peltier plate, then the temperature of the Peltier plate was changed from 4°C to 37°C, a

sinusoidal shear strain with 1% strain and 1 Hz frequency was applied to the sample, and the storage modulus (G') of the samples was recorded with time. To evaluate the storability of hydrogels, the alginate or hydrogel precursor solutions were stored at 4°C for 28 days. At days 0, 7, 14, and 28, the precursor solutions were mixed to make alg/col 1/1 hydrogel and the viscosity and G' were measured as described above. Injectability of the alg/col hydrogels was also tested via loading the gel into a 1 mm syringe (Norm-Ject syringe, Air-Tite Products Co., Inc., Virginia Beach, VA) and manual injection of the gel through a 20G needle (PrecisionGlide, Becton Dickinson, Franklin Lakes, NJ) onto wells of a 6-well plate. The injected strut was imaged using a Zeiss AxioObserver Z1 microscope.

2.2.3. Scanning electron microscopy (SEM) imaging—The alg/col hydrogels samples were immersed in liquid nitrogen and freeze-dried. The freeze-dried samples were dipped in liquid nitrogen and cut using a surgical blade, as described elsewhere [42]. The hydrogel samples were then coated with gold using a SPI sputter (SPI Supplier Division of Structure Prob, Inc., West Chester, PA) for 180 seconds and imaged using a Field Emission Scanning Electron Microscope (Zeiss Sigma, White Plains, NY) at an accelerating voltage of 5 keV.

2.2.4. Fluorescent imaging—For alginate fluorescent labeling, 500 mg of alginate was dissolved in 50 mL MES buffer (100 mM) containing EDC (1 mg/mL) and NHS (1 mg/mL) and allowed to react for 30 min at room temperature to activate the carboxylic acid groups. 5 mg of 5-(Aminomethyl)Fluorescein dye was dissolved in 100 μL DMSO, mixed with the activated alginate solution and stirred for 2 hr at room temperature in dark. The solution of stained alginate (s-alg) was then dialyzed against DI water using a dialysis tube (Spectrum Laboratories, Rancho Dominquez, CA) with 6−8 kDa molecular weight cutoff for 3 days at ambient temperature.

To stain collagen, 1 mg of Texas Red™-X, Succinimidyl Ester dye was dissolved in 100 μL DMSO and then diluted in 5 mL PBS. 100 μL of alg/col hydrogel or pure collagen hydrogel was injected onto wells of a 24-well plate, incubated at 37°C for 30 minutes, and was thoroughly washed with PBS five times. Then, the dye solution was added to the hydrogel samples and incubated at room temperature in dark for 2 hr. The hydrogel samples were then washed with PBS five times (each time 30 min incubation at room temperature in dark) to fully remove the unreacted dye. The stained alg/col hydrogels were imaged using a Zeiss AxioObserver Z1 fluorescent microscope.

2.2.5. Measurement of mass loss—In order to measure the degradation kinetics of alg/col hydrogels, 2 mL of alg/col 1/0.25, alg/col 1/0.5 or alg/col 1/1 hydrogels was injected into Teflon molds and incubated at 37°C for 30 minutes. Each sample was then transferred to a tube with 20 mL PBS supplemented with collagenase (1 μg/mL) and sodium citrate (20 μg /mL) and incubated at 37 °C under mild agitation. The reported concentrations of collagenase and citrate in synovial fluid and plasma are in the order of 1 μg/mL, and 20 μg /mL, respectively [43, 44]. At each time point, the tubes were centrifuged at 2000×g, the supernatant was removed, and the samples were lyophilized. The weight of dried samples was measured and compared with the weight of dried samples at day 0 to determine the fractional mass loss at each time point.

2.2.6. Protein release—Bovine serum albumin (BSA, 1% w/v) or BMP2 (20 μg/mL) was encapsulated in alg/col 1/0.25, alg/col 1/0.5 and alg/col 1/1 hydrogels. 100 μL of the BSA loaded or BMP2 loaded hydrogels or hydrogels without encapsulated protein (control groups) was injected onto wells of a 24-well plate and incubated at 37°C for 30 minutes. Then, 1 mL PBS was added to each well and the plate was incubated at 37°C for 14 days or 21 days. At each time point, the release medium was removed from the plates and replaced with fresh PBS. The removed release medium was transferred to siliconized microcentrifuge tubes and stored in a −80°C freezer. After collecting the release media at all time points, the total protein content or the BMP2 content was measured with BCA Protein Assay Kit (Thermo Fisher Scientific), or human BMP2 ELISA kit (Sigma-Aldrich), respectively according to manufacturer's instructions. The normalized released BSA at each time point was calculated by subtracting the protein released from BSA-laden samples from that of the control samples. The protein release tests were done in triplicate.

2.2.7. hMSCs culture—Human Mesenchymal Stem Cells (hMSCs) were cultured in DMEM medium (Life Technologies, USA) supplemented with 10% fetal bovine serum (FBS, Life Technologies, USA) and 1% Penicillin and Streptomycin (hereafter referred to as basal medium) at 37°C in a 5% CO_2 humidified incubator. After reaching 70% confluency, hMSCs were enzymatically lifted with trypsin-EDTA and used for in-vitro studies. All cells were passaged < 6 times prior to the in-vitro studies.

2.2.8. Viability and proliferation of hMSCs in alg/col hydrogels—For cell encapsulation, 0.5, 1 or 5 million hMSCs were suspended in 500 μL collagen precursor solutions with different alg/col ratios or $CaSO_4$ content. The collagen precursor solution was then added to 500 μL of sterile alginate precursor solution and mixed gently via pipetting. 50 μL of the hMSC-laden hydrogel was injected onto wells of a 24-well plate and incubated at 37°C for 30 minutes. The hydrogels were then incubated in 1 mL of basal medium at 37°C and 5% CO_2. For cell viability measurement, gels were stained with Calcein AM (2 μM) and Ethidium homodimer-1(4 μM) to image live and dead hMSCs according to manufacturer's instructions and imaged using a Zeiss AxioObserver Z1 fluorescent microscope. The live/dead images were divided into smaller squares and the number of live and dead cells were counted manually to calculate the cell viability, as described elsewhere [45]. To quantify the DNA content of the cell encapsulated hydrogel sample, at each time point, the samples were transferred into new wells and incubated in 500 μL of DMEM medium supplemented with collagenase (1 mg/mL) for 1 hour at 37°C. Then, 250 μL of 3% triton solution in PBS was added to each well and the attached cells were lifted from the surface using a CytoOne cell scraper (USA Scientific Inc, Ocala, FL). Then the cell suspension was transferred to a microcentrifuge tube and sonicated to rupture the cell membrane. The lysate was centrifuged at 2000×g for 15 min at 4°C and the supernatant was collected. The content of double-stranded DNA in the supernatant was measured using Quant-iT PicoGreen DNA assay according to manufacturer's instructions [42].

2.2.9. Osteogenic differentiation of hMSCs in alg/col hydrogels—For osteogenic differentiation, 50 μL of hMSC-laden alg/col hydrogel with 0.5, 1 or 5 million cells/mL was injected onto wells of a 24-well plate and incubated in 1 mL of basal medium

at 37°C and 5% CO_2. After 24 hr, the medium was replaced with osteogenic medium (basal medium supplemented with 100 nM dexamethasone, 50 μg/mL ascorbic acid, 10 mM β-sodium glycerophosphate) or fresh basal medium (control groups) and incubated for 28 days [46]. To measure ALP activity, at each time point (0, 7, 14, 21, and 28 days), hydrogel samples were transferred into new wells and incubated in 500 μL of DMEM medium supplemented with collagenase (1 mg/mL) for 1 hour at 37°C to digest the gels. Then, 250 μL of 3% triton solution in PBS was added to each well and the attached cells were lifted from the surface using a cell scraper. Then the cell suspension was transferred to a microcentrifuge tube and sonicated. The lysate was centrifuged at 2000×g for 15 min at 4°C and the supernatant was collected. The ALP activity in the supernatant was measured using QuantiChrom ALP assay kit according to the manufacturer's Instructions, on the plate reader at 405 nm. To measure the calcium content, hMSC-laden hydrogel samples were first lysed as described above. Then, 250 μL of 1N HCL solution was added to the lysate and mixed overnight at 4°C as described [47]. Next, the lysate was centrifuged at 2000×g for 15 min at 4°C and the supernatant was collected. The calcium content in the supernatant was measured using QuantiChrom Calcium assay kit on the plate reader at 612 nm. The ALP activity and calcium content at each time point were normalized by dividing by the DNA content at that time point. To visualize the mineralization, at day 28, the hMSC-laden gels were washed 3 times with PBS, stained with Alizarin red and imaged using a Zeiss AxioObserver Z1 microscope [48].

2.2.10. In vivo calvarial bone defect repair—10-week-old male Sprague–Dawley (SD) rats (Charles River Laboratories, Wilmington, MA) were used in this study. The animal surgery protocol was approved by the Institutional Animal Care and Use Committee (IACUC) at Stanford University and was in accordance with the National Institute of Health (NIH)'s guidelines [49]. All surgeries were performed under anesthesia, and Buprenorphine Sustained-Release (SR) was administered to minimize the suffering of animals. The operation procedure was modified based on the previous publications [50, 51]. Each rat was anaesthetized with 2–3% isoflurane during operation on a heated platform. After disinfection, a 15-mm incision was made along the sagittal mid-line to expose the sagittal suture and coronal suture. The periosteum was carefully incised along the sagittal suture to expose the calvarial bone. Then a defect with 8-mm in diameter with its center in the middle of the sagittal suture was created using a trephine drill (Dentium, Suwon, Korea) with normal saline irrigation during processing. Then 100 μL alg/col 1/0.5 hydrogel with or without 2μg BMP2 (n = 6 per time point per group) was injected to the calvarial defect site. The animals with a defect only were regarded as negative controls (Blank control; n = 6 per time point). The hydrogel was secured by suturing periosteum and skin sequentially. The rats were sacrificed after 4 or 8 weeks, and samples were harvested for the following micro-computed tomography (micro-CT) analysis.

2.2.11. Micro-CT analysis—The collected rat calvarial specimens were fixed in 10% buffered formalin and then preserved in 70% ethyl alcohol for bone scanning using a Skyscan 1276 micro-CT (Bruker, Kontich, Belgium) as previously described [52, 53]. The scanning was performed with a custom isotropic resolution of 20 μm isometric voxel size with a voltage of 70 kV and a current of 200 μA, with a rotation step of 0.8° and in 360°

scan mode. Beam hardening reduction was applied using a 0.5 mm Al filter. The projection images were reconstructed offline using a cone beam NRecon application (version 1.0.7.0., Bruker) with post-alignment and beam hardening corrections for image analysis. Post processing of the reconstructed images was analyzed using the SkyScan CTAn software package (version, 1.17, Bruker). Regions of interest (ROIs) were defined as the full thickness of 8-mm calvarial defect site. All the slices with bone were selected to create a volume of interest (VOI) to generate the bone volume/ tissue volume fraction (BV/TV) measured by Ctan with the threshold of bone ranging from 80 to 255 g/cm3. Data were normalized by the mean value of BV/TV of the intact calvarial bone controls. 3D bone structure was made from the segmented dataset with CTAn (CT Hounsfield units (HU) threshold >10000) for visual inspection using the MicroView 3D Image Viewer (Version 2.5.0, Parallax Innovations Inc., Ilderton, Canada).

2.2.12. Histology and immunohistochemistry—Immediately after micro-CT scanning, the specimens (n = 6 per group) were decalcified in 10 % EDTA solution for 4 weeks and embedded in optimal cutting temperature (OCT; Fisher HealthCare, Waltham, MA). Thin sections (5 μm) were cut by a rotary cryostat (HM525 NX; Thermo Fisher Scientific, Waltham, MA) from the sagittal suture of each cranial bone in the sagittal plane. After washing, the slides were stained with hematoxylin and eosin (H & E; Sigma-Aldrich, St Louis, MA) and Trichrome stain kit (Abcam, Cambridge, MA) for observation under microscope. The expressions of osteocalcin (OCN) and osteopontin (OPN) in the defect sites were measured by immunohistochemistry. The slides (n = 6) were incubated with primary antibodies against OCN (1:100; Santa Cruz, CA) or OPN (1:100; Santa Cruz, CA) and subsequently with horseradish peroxidase (HRP)-conjugated secondary antibody (1:200; Santa Cruz, CA). Primary antibody was replaced with blocking solution in the negative controls. The sections were examined under light microscopy. ImageJ (NIH) was introduced to analyze the OCN- or OPN-positive area in the defect sites.

2.2.13. Statistical analysis—All experiments were done in triplicate. Statistically significant differences between groups were tested using a two-way ANOVA with replication, followed by a two-tailed Students t-test. A p-value smaller than 0.05 ($p < 0.05$) was considered statistically significant.

3. Results

The effect of shear rate on the viscosity of alginate (alg, blue line), collagen (col, green line), alg/col 1/0.25 (brown line), alg/col 1/0.5 (red line), and alg/col 1/1 (purple line) hydrogels is shown in Figure 2a. At the minimum shear rate (0.13 1/s), the viscosities of alg/col hydrogels were significantly higher than that of alginate or collagen. The viscosity of alg/col hydrogels at minimum shear rate increased by 3.4, 5.9 and 7.9 folds when the collagen to alginate weight ratio increased from 0 to 0.25, 0.5, and 1, respectively. The viscosities of all hydrogels decreased when the shear rate increased from 0.13 to 48 (1/s). The shear-thinning characteristics indicated injectability of alg/col hydrogels regardless of the alginate to collagen ratio [54].

The effect of alginate to collagen weight ratio on the evolution of storage modulus of the alg/col hydrogels with time at 37 °C is shown in Figure 2b. The storage modulus of alginate gel (blue markers) did not significantly change but the storage modulus of collagen (green markers) increased by 2.1 folds over 900 seconds at 37 °C. The storage modulus of alg/col 1/0.25 (brown markers), alg/col 1/0.5 (red markers), and alg/col 1/1 (purple markers) gels raised by 1.6, 1.6, and 1.2 folds, respectively after 900 seconds at 37 °C. The storage moduli of alg/col hydrogels were significantly higher than those of alginate gel or collagen over 900s. The storage modulus of alg/col gels after 900 seconds (Figure 2c) increased from 23 Pa to 224 Pa, 985 Pa, and 1560 Pa with increasing the collagen to alginate weight ratio from 0 to 0.25, 0.5, and 1.

The effect of $CaSO_4$ concentration on the growth of storage modulus of alg/col 1/0.5 hydrogels at 37 °C is shown in Figure 2d. The storage modulus of alg/col 1/0.5 gels increased by 1.8, 1.6, 1.6 or 1.3 folds over 900 seconds at 37 °C when the $CaSO_4$ concentration was 0, 0.5, 1, or 1.5 (mg/mL), respectively. The storage modulus of alg/col 1/0.5 hydrogel at any time significantly increased with increasing the $CaSO_4$ concentration. For instance, after 900 seconds, the storage modulus of alg/col 1/0.5 hydrogel (Figure 2e) increased from 105 to 223, 984, and 1402 with changing the $CaSO_4$ concentration from 0 to 0.5, 1, and 1.5 (mg/mL).

Figure 2f shows the effect of storage time of precursor solutions on the shear dependent viscosity of the alg/col 1/0.5 hydrogel. A decreasing trend in the viscosity of hydrogel with increasing the shear rate was not significantly impacted by the storage of precursor solutions for 28 days at 4°C. The viscosity of the alg/col 1/0.5 hydrogel that was prepared from precursor solutions after 28 days of storage (Figure S1a, 28 days) at 0.1, 1, or 10 (1/s) shear rates was not statistically significant different from that of alg/col 1/0.5 hydrogel made from fresh precursor solutions (Figure S1a, 0 days). Further, the storage modulus of the alg/col 1/0.5 hydrogel after 900 seconds at 37°C did not significantly change with storing the precursor solutions for 7, 14, or 28 days (Figure S1b).

In addition to rheological characterization, the injectability of the alg/col hydrogels was also tested via manual injection of the gels through a 20G needle. Figure 3a shows an alg/col 1/0.5 gel strut injected from a 20G needle. The average strut thickness was 810 μm which was slightly higher than the nominal inner diameter of a 20G needle (600 μm) [55]. The alginate to collagen weight ratio and the concentration of $CaSO_4$ did not significantly impact the injectability of the gel or the injected strut thickness (data not shown). A representative SEM image of alg/col 1/0.5 hydrogel is shown in Figure 3b. The hydrogel samples had a porous microstructure with average pore size of 15 μm.

The distribution of alginate and collagen in alg/col hydrogels was evaluated via fluorescent imaging. Figure 3c shows a fluorescent image of alg hydrogel (without collagen) that was prepared with green fluorescent-labeled alginate. The alginate in the absence of collagen was evenly distributed in the hydrogel indicated by a uniform green color in Figure 3c. A fluorescent image of col hydrogel (without alginate) stained with red fluorescent dye is shown in Figure 3d. The collagen in the absence of alginate was evenly dispersed in the hydrogel. Figure 3e shows a fluorescent image of alg/col 1/0.5 hydrogel that was prepared

with green fluorescent-labeled alginate and then stained with red fluorescent dye to visualize collagen. The orange color indicated that both alginate hydrogel and collagen hydrogel contributed to the network and alginate gelation did not negatively impact the collagen network formation.

The degradation kinetics of alg/col hydrogels over 21 days at 37 °C in PBS supplemented with collagenase and sodium citrate is shown in Figure 3f. The remaining mass of alg/col 1/0.25, alg/col 1/0.5, and alg/col 1/1 hydrogels monotonically decreased from 100% at day 0 to 10.5%, 9.0%, and 20.5% at day 21, respectively. The remaining mass of alg/col 1/1 was significantly higher than that of alg/col 1/0.25 hydrogel after 14 or 21 days. The release kinetics of BSA from alg/col hydrogels is shown in Figure 3g. Following an initial burst release in the first day, the BSA release was slower from day 1 to 5 and reached a plateau after day 5. The amount of released BSA from alg/col hydrogels at 24 hr and 72 hr significantly decreased with increasing the alginate to collagen ratio. For instance, the amount of released BSA at 24hr decreased significantly from 66.8% to 59.7% and 50.2% with changing the alginate to collagen weight ratio from 1/0.25 to 1/0.5, and 1/1. The amount of released BSA from alg/col hydrogels after 120 hr was over 90%. Also, alginate to collagen ratio did not significantly influence the amount of released BSA at 120 hr, 240 hr or 336 hr time points. The BMP2 release from alg/col hydrogels had a fast rate in the first 3 days in the range of 63.6% to 74.5% followed by a slower rate from day 3 to 14, accounting for 93.7% to 95.7% in total (Figure 3h). The amount of released BMP2 from the alg/col hydrogels did not significantly change after day 14. At day 1 and day 3, the amount of released BMP2 from alg/col 1/0.25 hydrogel was significantly higher than the amount of BMP2 released from alg/col 1/0.5 or alg/col 1/1 hydrogels. After day 3, there was not a significant difference between the amount of BMP2 released from different hydrogels. Also, the released BMP2 from alg/col 1/0.5 and alg/col 1/1 hydrogels were not significantly different at any time point.

Figure 4a, 4b, and 4c show images of live (green) and dead (orange) hMSCs encapsulated in alg/col 1/0.5 hydrogel with 0.5, 1 and 5 million cells/mL densities, respectively 24hr after encapsulation. The viability of hMSCs encapsulated in alg/col 1/0.5 hydrogel after 24hr was 94%, 92%, and 93% for 0.5, 1 and 5 million cells/mL cell densities. The live/dead images of hMSCs-laden alg/col 1/0.5 hydrogel with 0.5, 1 and 5 million cells/mL densities, after 0, 7, and 14 days of incubation are shown in Figure S2. The viability of hMSCs for all cell densities remained over 90% at day 7 and 14. The effect of alginate to collagen weight ratio on the viability of hMSCs encapsulated in alg/col hydrogel with 1 million cells/mL density after 24hr is shown in Figure 4d. The hMSC viability was 94%, 92%, and 95% for alg/col 1/0.25, alg/col 1/0.5, and alg/col 1/1 hydrogels, respectively. The variation in cell viability in alg/col hydrogels with changing the alginate to collagen ratio was not statistically significant. Figure 4e shows the effect of $CaSO_4$ concentration in alg/col 1/0.5 hydrogels on the viability of encapsulated hMSCs. The viability of hMSCs encapsulated in alg/col 1/0.5 hydrogel with 0.5, 1 or 1.5 mg/mL $CaSO_4$ concentration did not significantly change from day 1 to 7. Further, a change in the $CaSO_4$ concentration from 0.5 to 1 or 1.5 mg/mL did not significantly affect the hMSC viability at day 1, 3 or 7. DNA content of hMSC-laden alg/col 1/0.5 hydrogels with cell densities of 0.5, 1 and 5 million cells/mL cultured in basal medium over 28 days is shown in Figure 4f. When the density of hMSCs in alg/col hydrogel was 0.5

million cells/mL (0.5 m, blue line) the DNA content increased by 37.2 folds from day 0 to 28. The DNA content of alg/col hydrogel with 1 million encapsulated hMSCs/mL (1m, red line) increased by 26.8 folds from day 0 to day 21 and then did not significantly change from day 21 to 28. The DNA content of alg/col hydrogel with 5 million hMSCs/mL (5 m, green line) initially increased by 6.2 folds from day 0 to 14 and then slightly dropped from day 14 to 28.

Images in Figure 5a show Alizarin red stained hMSC-laden alg/col 1/0.5 hydrogels with 0.5, 1 and 5 million cells/mL densities and incubated in basal medium (BM) or osteogenic medium (OM) for 28 days. A significantly higher mineralization was observed in hMSC-laden hydrogel groups that were incubated in OM compared to those incubated in BM. ALP activity of hMSCs encapsulated in alg/col 1/0.5 hydrogels with 0.5, 1, or 5 million cells/mL density and incubated in BM or OM for 28 days is shown in Figure 5b. The ALP activity of hMSCs did not significantly change when the cell-laden alg/col hydrogels were incubated in BM. The ALP activity of hMSCs encapsulated in alg/col hydrogels and incubated in OM drastically increased from day 0 to 14 and then either dropped (for 1 and 5 million cells/mL densities) or did not significantly change (for 0.5 million cells/mL density) from day 14 to 28.

Calcium content of alg/col 1/0.5 hydrogels loaded with 0.5, 1, or 5 million hMSCs/mL and incubated in BM or OM for 28 days is shown in Figure 5c. The calcium content of hydrogel samples did not significantly change when the hMSC-laden alg/col hydrogels were incubated in BM, regardless of cell density. The calcium content of those hMSC-laden hydrogels that were incubated in OM did not change initially from day 0 to 7, then significantly increased from day 7 to 28. The calcium content of hMSC-laden hydrogels with 1 or 5 million cells/mL cell density was significantly higher than that of hMSC-laden hydrogels with 0.5 million cells/mL after 28 days of incubation in OM.

The efficacy of the BMP2-incorporated alg/col 1/0.5 hydrogel in calvarial bone defect healing was assessed by micro-CT analysis at 4 weeks or 8 weeks after implantation. From the 3D reconstructed results, we found only small amount of new bone regenerated from the cutting edges in the blank control group and in the hydrogel only group at 4 weeks or 8 weeks (Figure 6a). The hydrogel alone showed no significant effect on bone healing compared with blank controls (Figure 6a and 6b). However, the hydrogel loaded with BMP2 promoted calvarial bone healing significantly, with 135.8% ($P < 0.05$) or 190.8% ($P < 0.001$) increase in bone volume fraction (BV/TV) after 4 weeks or 8 weeks respectively, compared with the blank control group. In addition, the bone volume fraction of BMP2-laden hydrogel group was 91.3% ($P < 0.05$) or 207.8% ($P < 0.001$) higher after 4 weeks or 8 weeks, compared with that of the hydrogel only group (Figure 6a and 6b). After 8 weeks of BMP2-laden hydrogel injection, the calvarial bone defect nearly healed, with a 56.3% ($P < 0.05$) increase in BV/TV compared with that after 4 weeks of injection (Figure 6a and 6b).

Histological results (Figure 7 and Figure S3) showed regenerated tissue in the calvarial defect sites and an integration of newly formed tissue with the existing native tissue at 4 or 8 weeks after implantation (Figure 7). From the results of Trichrome and H & E staining, we found the defect sites were mainly covered with fibrous tissue and a few small bone islands

in the blank control group or hydrogel only group (alg/col 1/0.5 hydrogel) at 4 or 8 weeks after operation (Figure 7 and Figure S3). A large amount of newly formed bone with seamless integration to the native tissue at the defect sites was found in the BMP2-incorporated hydrogel (alg/col 1/0.5 hydrogel) group at 4 or 8 weeks after operation (Figure 7 and Figure S3). The newly formed bone in the later time point (8 weeks) was more mature than that at the early time point (4 weeks). This result was consistent with the data from micro-CT analysis, which showed a better bone healing effect in the BMP2-incorporated hydrogel group, especially at the later time point (8 weeks). Osteogenic markers including osteocalcin (OCN) and osteopontin (OPN) were measured by immunohistochemistry (Figure 8). As shown by the results, the expression levels of OCN and OPN were relatively low in the blank control group or hydrogel only group (alg/col 1/0.5 hydrogel) at 4 or 8 weeks after operation (Figure 8A–8C). However, significantly higher expression levels were found in the BMP2-laden hydrogel group, with 327.2% ($P < 0.001$) or 228.6% ($P < 0.001$) increase in percentage of OCN positive area, and 407.5% ($P < 0.001$) or 243.4% ($P < 0.001$) increase in percentages of OPN positive area after 4 weeks or 8 weeks, respectively, compared with the blank control group (Figure 8B and 8C). In addition, when compared with the hydrogel only group, the BMP2-laden hydrogel group had 285.5% ($P < 0.05$) or 228.6% ($P < 0.001$) higher percentage of OCN positive area, and 160.9% ($P < 0.001$) or 208.5% ($P < 0.001$) higher percentage of OPN positive area after 4 weeks or 8 weeks (Figure 8B and 8C).

4. Discussion

Collagen solution is an injectable liquid that crosslinks at 37°C and physiological pH and loses its injectability following crosslinking [30]. A potential dilution with body fluid, leakage to neighboring tissues and a chance of being washed away before gelation limit the use of uncrosslinked collagen solution for cell and/or protein delivery in regenerative medicine [6]. In addition, a low viscosity and inferior structural stability of collagen precursor solution, limits its application as bioink in 3D bioprinting [34]. In this work, we described a facile method to make injectable yet in-situ stable collagen-based hydrogels. The alg/col hydrogel preparation involved an alginate precursor solution and a collagen/$CaSO_4$ precursor solution. Two precursor solutions could be stored at 4°C and pipette mixed before use, as opposed to previously reported methods to make collagen/alginate-based hydrogels that necessitated using a post-injection crosslinking in $CaCl_2$ solution, a collagen pre-processing step and/or special instruments such as coaxial nozzles and luer-lock syringes [35–38]. Our results indicated that the viscoelastic characteristics and injectability of the alg/col hydrogels were not significantly impacted by the storage of precursor solutions for 28 days. Therefore, the precursor solutions could be stored and shipped at 4°C, and mixed right before use.

The storage modulus and viscosity of alginate hydrogel at 4°C (see Figure 2a and initial values in Figure 2b and 2d) increased with incorporation of collagen into the hydrogel and increasing the collagen concentration. Since collagen is not crosslinked at 4°C, the higher storage modulus and viscosity of alginate hydrogel in the presence of collagen might be due to an interaction between collagen and alginate and/or collagen and calcium ions as reported elsewhere [56, 57]. For example, an alginate-based hydrogel was made by crosslinking a

precursor solution containing alginate and hyaluronic acid using $CaCl_2$ [56]. The storage modulus and glass transition temperature (Tg) of alginate-based hydrogels increased when collagen was added to the precursor solution due to a potential chemical interaction between alginate and collagen [56].

According to the results, the storage modulus of crosslinked pure alginate hydrogel did not alter when the temperature was changed from 4°C to 37 °C, as opposed to pure collagen hydrogel with a growth in the storage modulus (see Figure 2 and results). Therefore, a time dependent growth in the storage modulus of the alg/col hydrogels at 37 °C was attributed to the collagen crosslinking within a precrosslinked alginate matrix. Also, the storage modulus of fully crosslinked alg/col hydrogels was significantly higher than that of pure alginate hydrogel (Figure 2c). An increase in the storage modulus of alginate hydrogel with addition of other ECM-based matrices has been reported elsewhere. For example, it was shown that the storage modulus of alginate based hydrogels at room temperature increased when the hydrogel precursor solution was blended with Matrigel [58].

The storage modulus of pure collagen hydrogel (2.5 mg/mL) in this work was 110 Pa that is the range of collagen hydrogel storage moduli reported elsewhere [59]. The storage modulus of pure collagen hydrogel is concentration dependent and increases with collagen concentration (c_{col}) with $c_{col}^{2.1}$ at 37°C [59]. Therefore, the storage modulus of pure collagen hydrogel increases by 4.3 folds, when c_{col} doubles. Results of this study showed when c_{col} in alg/col matrices doubled from 1.25 mg/mL (alg/col 1/0.25) to 2.5 mg/mL (alg/col 1/0.5), the storage modulus of the alg/col hydrogel increased by 4.4 folds. However, the storage modulus of alg/col hydrogels increased by only 1.6 folds when c_{col} doubled from 2.5 mg/mL (alg/col 1/0.5) to 5 mg/mL (alg/col 1/1). A smaller rate of growth in storage modulus of alg/col 1/1 hydrogel with c_{col} compared to that of alg/col 1/0.25, or alg/col 1/0.5 hydrogels (see Figure 2 and results) indicated a more pronounced impact of alginate and $CaSO_4$ on collagen crosslinking at high c_{col} (5 mg/mL). A higher initial viscosity (see Figure 2a) might hinder the collagen macromolecular motion and crosslinking at high collagen concentrations [60].

An increase in the storage modulus of alg/col hydrogels with $CaSO_4$ concentration was due to a raise in the Ca^{2+}-driven crosslinking density of alginate [61]. Also, an interaction between calcium ions and collagen might contribute to concentration-dependent increase in storage modulus of alg/col hydrogels with $CaSO_4$ concentration. It was shown that collagen molecules chelate calcium ions due to an electrostatic interaction between the negatively charged carboxyl groups on the collagen molecules and positively charged calcium ions and the elastic modulus of collagen fibrils increases with calcium ion concentration [57].

The viability of cells encapsulated in alg/col hydrogels was comparable with or higher than cell viability in alginate-based or collagen-based hydrogels reported elsewhere. For instance, the viability of placenta-derived MSCs in collagen hydrogels was over 90% after 24 hours of incubation [62]. The viability of MSCs in RGD peptide-modified injectable alginate hydrogel was around 90% [9]. MSC-loaded core-shell alginate/collagen fibrous hydrogels were made via injection of the precursor solutions through a concentric nozzle into a bath of $CaCl_2$ [38]. The viability of MSCs in the core-shell alginate/collagen hydrogel was around

70% after 7 days [38]. Results of this study showed that the viability of hMSCs in injected alg/col hydrogels was over 90% during 7 days of incubation, irrespective of the alginate/collagen ratio or $CaSO_4$ concentration. It was shown elsewhere that the viability of hMSCs in collagen-based hydrogels was not significantly affected when the collagen content was changed from 1mg/mL to 3mg/mL [63]. The results of this work similarly showed the viability of hMSCs in alg/col hydrogel was not significantly changed with variation of collagen content (alg/col ratio) (Figure 4d). It is known that a low concentration of calcium ion (~2mM) is vital for cell survival but exposure of cells encapsulated in alginate-based hydrogels to a high concentration of calcium ion (>100 mM) has a negative impact on cell viability [64]. The concentration of calcium ion in the alg/col hydrogels in this work ranged between 3.7 to 11 mM (0.5 to 1.5 mg/mL $CaSO_4$) and did not have a significant impact on the viability of hMSCs (Figure 4e). The results of this study also revealed that the variation of alg/col hydrogel stiffness in 224–1560 Pa range (Figure 2) did not have an impact on viability of encapsulated hMSC viability (Figure 4d and 4e).

A continuous proliferation of MSCs in collagen-based matrices were previously reported. For example, the number of rat MSCs encapsulated in collagen hydrogel (10^5 cells/mL initial cell density) monotonically increased over 21 days with 3 folds growth from day 7 to 21 [38]. In contrast, the number of hMSCs encapsulated in RGD peptide-grafted alginate hydrogels ($2–20\times10^6$ cells/mL initial cell density) did not grow in two weeks [65, 66]. Results of this study showed the number of hMSCs in alg/col hydrogels during 28 days of incubation raised by 6.2 to 37.2 folds depending on the initial cell density ($0.5–5\times10^6$ cells/mL). The DNA content of hMSCs in alg/col hydrogels reached a plateau corresponding to around 30 million cells/mL that could be interpreted as the highest cell density within alg/col hydrogels.

We further showed that osteo-inductive conditions stimulated osteogenic differentiation of hMSCs in alg/col hydrogels at all studied cell densities (0.5, 1, 5 million cells/mL). Osteogenic differentiation of MSCs in alginate or collagen-based matrices under osteo-inductive conditions has been reported elsewhere. For instance, osteogenic medium induced osteogenic differentiation of hMSCs in RGD-grafted alginate hydrogels and osteogenic differentiation was enhanced when the initial cell density in the hydrogel increased from 2 to 15 million cells/mL [65]. Osteogenic differentiation of MSCs in soft collagen-based hydrogels have been shown in several studies. For instance, osteogenic differentiation of rat MSC encapsulated in collagen hydrogels with 0.4–1.6 mg/mL collagen content was more pronounced than osteogenic differentiation rat MSCs cultured on 2D plates [67]. Another study reported a significantly higher osteogenic differentiation of hMSCs encapsulated in 3D collagen hydrogels compared to hMSCs seeded on 2D tissue culture plate under osteo-inductive conditions [68].

Osteo-inductive BMP2 was released from the alg/col hydrogel in 14 days in-vitro, while the release of BSA took 5 days. A slightly slower release of BMP2 compared with BSA might be due to a higher isoelectric index (pI) of BMP2 protein (8.5) compared with pI of BSA (4.7) in physiological pH, hence lower electrostatic repulsion between the negatively charged alginate and the BMP2 protein [69–71]. When the alg/col hydrogel was used as a carrier for sustained delivery of 2 μg osteo-inductive BMP2 to 8 mm calvarial bone defect in

rats, it promoted bone healing after 8 weeks of injection. The promoting effect of sustained BMP2 delivery in treatment of calvarial defect models has been reported in a number of studies. For instance, delivery of 5 μg BMP2 in injectable poly(phosphazene)-based hydrogels (sustained delivery) healed a 5 mm calvarial defect in mouse 8 weeks after injection, whereas treatment of the defect with 10 μg BMP2 in solution (without sustained release) did not heal the defect [55]. In another study, 2 μg BMP2 delivered in a hydrogel based on collagen microspheres and alginate healed a 5 mm calvarial defect model in rats while the hydrogel alone or the hydrogel with a lower BMP2 dose (0.2 μg) did not heal the defect [72].

The alg/col hydrogel was injectable through commercially available needles and the injected hydrogel was stable right after injection. The alg/col hydrogel was microporous, and degradable. In addition, the release kinetics of BMP2 and efficacy of the released BMP2 in bone healing indicated a potential application for alg/col hydrogels as injectable carriers for delivery of therapeutics for regeneration of tissues. Another potential application of alg/col hydrogels could be 3D culture or delivery of stem cells due to a high viability as well as proliferation and differentiation of encapsulated stem cells within alg/col hydrogels.

5. Conclusion

We developed a facile method to make pre-crosslinked injectable collagen-based hydrogels for delivery of cells and growth factors in regenerative medicine or bioprinting. The alg/col hydrogels were injectable, yet stable after injection due to pre-crosslinking. The precursor solutions of alg/col hydrogels were storable for 28 days at 4°C, and storage did not significantly impact the viscoelastic characteristics and injectability of the hydrogels. The viscosity and storage modulus of the alg/col hydrogels were tuned via changing the collagen content or $CaSO_4$ concertation in the hydrogel. The alg/col hydrogel was microporous and degradable. BSA and BMP2 proteins loaded into alg/col hydrogels were released in 5 days and 14 days, respectively. When the alg/col hydrogel was used as a carrier for sustained delivery of BMP2 to a calvarial bone defect in rats, it promoted bone healing after 8 weeks of injection. hMSCs encapsulated in alg/col hydrogels had over 90% viability and proliferated along 28 days of incubation. In addition, hMSCs encapsulated in alg/col hydrogels and incubated in osteogenic medium for 28 days were osteogenically differentiated and formed a mineralized matrix. The alg/col hydrogel could potentially be used for delivery of cells or biomolecules in surgeries or as bioink in bioprinting applications.

Supplementary Material

Refer to Web version on PubMed Central for supplementary material.

Acknowledgements

This research was funded through financial support from NIH grants R01AR057837, U01AR069395, R01AR072613, and R01AR074458 from NIAMS, and DoD grant W81XWH-20-1-0343. Dr. YoungBum Park is in charge of the in vivo study and a co-corresponding author for the animal experiments in this manuscript. The MicroCT (Bruker Skyscan 1276) instrument was purchased using NIH S10 Shared Instrumentation Grant (1S10OD02349701, PI Timothy C. Doyle).

Data availability

All data supporting the findings of this study are available within the paper and its supplementary file.

References

1. Jabbari E, Hydrogels for Cell Delivery. Gels, 2018 4(3).
2. Liu M, et al., Injectable hydrogels for cartilage and bone tissue engineering. Bone Research, 2017 5.
3. Munarin F, et al., New perspectives in cell delivery systems for tissue regeneration: natural-derived injectable hydrogels. Journal of Applied Biomaterials & Functional Materials, 2012 10(2): p. 67–81. [PubMed: 22865572]
4. Slaughter BV, et al., Hydrogels in Regenerative Medicine. Advanced Materials, 2009 21(32–33): p. 3307–3329. [PubMed: 20882499]
5. Li YL, Rodrigues J, and Tomas H, Injectable and biodegradable hydrogels: gelation, biodegradation and biomedical applications. Chemical Society Reviews, 2012 41(6): p. 2193–2221. [PubMed: 22116474]
6. Guvendiren M, Lu HD, and Burdick JA, Shear-thinning hydrogels for biomedical applications. Soft Matter, 2012 8(2): p. 260–272.
7. Yan C, et al., Injectable solid hydrogel: mechanism of shear-thinning and immediate recovery of injectable beta-hairpin peptide hydrogels. Soft Matter, 2010 6(20): p. 5143–5156. [PubMed: 21566690]
8. Ashammakhi N, et al., Minimally Invasive and Regenerative Therapeutics. Adv Mater, 2019 31(1): p. e1804041. [PubMed: 30565732]
9. Aguado BA, et al., Improving Viability of Stem Cells During Syringe Needle Flow Through the Design of Hydrogel Cell Carriers. Tissue Engineering Part A, 2012 18(7–8): p. 806–815. [PubMed: 22011213]
10. Bidarra SJ, Barrias CC, and Granja PL, Injectable alginate hydrogels for cell delivery in tissue engineering. Acta Biomater, 2014 10(4): p. 1646–62. [PubMed: 24334143]
11. Jalalvandi E and Shavandi A, Shear thinning/self-healing hydrogel based on natural polymers with secondary photocrosslinking for biomedical applications. J Mech Behav Biomed Mater, 2019 90: p. 191–201. [PubMed: 30368205]
12. Loebel C, et al., Shear-thinning and self-healing hydrogels as injectable therapeutics and for 3D-printing. Nat Protoc, 2017 12(8): p. 1521–1541. [PubMed: 28683063]
13. Samimi Gharaie S, Dabiri SMH, and Akbari M, Smart Shear-Thinning Hydrogels as Injectable Drug Delivery Systems. Polymers (Basel), 2018 10(12).
14. Rodell CB, et al., Injectable Shear-Thinning Hydrogels for Minimally Invasive Delivery to Infarcted Myocardium to Limit Left Ventricular Remodeling. Circ Cardiovasc Interv, 2016 9(10).
15. Augst AD, Kong HJ, and Mooney DJ, Alginate hydrogels as biomaterials. Macromol Biosci, 2006 6(8): p. 623–33. [PubMed: 16881042]
16. Lee KY and Mooney DJ, Alginate: properties and biomedical applications. Prog Polym Sci, 2012 37(1): p. 106–126. [PubMed: 22125349]
17. Kuo CK and Ma PX, Ionically crosslinked alginate hydrogels as scaffolds for tissue engineering: Part 1. Structure, gelation rate and mechanical properties. Biomaterials, 2001 22(6): p. 511–521. [PubMed: 11219714]
18. Espona-Noguera A, et al., Tunable injectable alginate-based hydrogel for cell therapy in Type 1 Diabetes Mellitus. International Journal of Biological Macromolecules, 2018 107: p. 1261–1269. [PubMed: 28962846]
19. Freeman FE and Kelly DJ, Tuning Alginate Bioink Stiffness and Composition for Controlled Growth Factor Delivery and to Spatially Direct MSC Fate within Bioprinted Tissues. Scientific Reports, 2017 7.
20. Dhoot NO, et al., Peptide-modified alginate surfaces as a growth permissive substrate for neurite outgrowth. Journal of Biomedical Materials Research Part A, 2004 71a(2): p. 191–200.
21. Hunt NC, et al., 3D culture of human pluripotent stem cells in RGD-alginate hydrogel improves retinal tissue development. Acta Biomaterialia, 2017 49: p. 329–343. [PubMed: 27826002]

22. Yu JS, et al., The use of human mesenchymal stem cells encapsulated in RGD modified alginate microspheres in the repair of myocardial infarction in the rat. Biomaterials, 2010 31(27): p. 7012–7020. [PubMed: 20566215]
23. Akiyama SK, Aota S, and Yamada KM, Function and Receptor Specificity of a Minimal 20-Kilodalton Cell Adhesive Fragment of Fibronectin. Cell Adhesion and Communication, 1995 3(1): p. 13–25. [PubMed: 7538414]
24. Custodio CA, et al., Immobilization of fibronectin in chitosan substrates improves cell adhesion and proliferation. Journal of Tissue Engineering and Regenerative Medicine, 2010 4(4): p. 316–323. [PubMed: 20049746]
25. Gelse K, Poschl E, and Aigner T, Collagens - structure, function, and biosynthesis. Advanced Drug Delivery Reviews, 2003 55(12): p. 1531–1546. [PubMed: 14623400]
26. Sweeney SM, et al., Candidate cell and matrix interaction domains on the collagen fibril, the predominant protein of vertebrates. Journal of Biological Chemistry, 2008 283(30): p. 21187–21197.
27. Zeltz C and Gullberg D, The integrin-collagen connection - a glue for tissue repair? Journal of Cell Science, 2016 129(4): p. 653–664. [PubMed: 26857815]
28. Ni YL, et al., Collagen structure regulates MSCs behavior by MMPs involved cell-matrix interactions. Journal of Materials Chemistry B, 2018 6(2): p. 312–326. [PubMed: 32254173]
29. Popov C, et al., Integrins alpha 2 beta 1 and alpha 11 beta 1 regulate the survival of mesenchymal stem cells on collagen I. Cell Death & Disease, 2011 2.
30. Antoine EE, Vlachos PP, and Rylander MN, Review of Collagen I Hydrogels for Bioengineered Tissue Microenvironments: Characterization of Mechanics, Structure, and Transport. Tissue Engineering Part B-Reviews, 2014 20(6): p. 683–696. [PubMed: 24923709]
31. Antoine EE, Vlachos PP, and Rylander MN, Tunable Collagen I Hydrogels for Engineered Physiological Tissue Micro-Environments. Plos One, 2015 10(3).
32. Dai WD, et al., Delivering stem cells to the heart in a collagen matrix reduces relocation of cells to other organs as assessed by nanoparticle technology. Regenerative Medicine, 2009 4(3): p. 387–395. [PubMed: 19438314]
33. Youngblood RL, et al., It's All in the Delivery: Designing Hydrogels for Cell and Non-viral Gene Therapies. Molecular Therapy, 2018 26(9): p. 2087–2106. [PubMed: 30107997]
34. Zhang YS, et al., 3D Bioprinting for Tissue and Organ Fabrication. Annals of Biomedical Engineering, 2017 45(1): p. 148–163. [PubMed: 27126775]
35. Ali Z, et al., Adjustable delivery of pro-angiogenic FGF-2 by alginate:collagen microspheres. Biol Open, 2018 7(3).
36. Baniasadi M and Minary-Jolandan M, Alginate-Collagen Fibril Composite Hydrogel. Materials, 2015 8(2): p. 799–814. [PubMed: 28787971]
37. Bendtsen ST and Wei M, Synthesis and characterization of a novel injectable alginate-collagen-hydroxyapatite hydrogel for bone tissue regeneration. Journal of Materials Chemistry B, 2015 3(15): p. 3081–3090. [PubMed: 32262508]
38. Perez RA, et al., Utilizing Core-Shell Fibrous Collagen-Alginate Hydrogel Cell Delivery System for Bone Tissue Engineering. Tissue Engineering Part A, 2014 20(1–2): p. 103–114. [PubMed: 23924353]
39. Lee HJ, et al., A New Approach for Fabricating Collagen/ECM-Based Bioinks Using Preosteoblasts and Human Adipose Stem Cells. Adv Healthc Mater, 2015 4(9): p. 1359–68. [PubMed: 25874573]
40. Su W, et al., Alginate-Assisted Mineralization of Collagen by Collagen Reconstitution and Calcium Phosphate Formation. ACS Biomaterials Science & Engineering, 2020 6(6): p. 3275–3286.
41. Bruyas A, et al., Effect of Electron Beam Sterilization on Three-Dimensional-Printed Polycaprolactone/Beta-Tricalcium Phosphate Scaffolds for Bone Tissue Engineering. Tissue Engineering Part A, 2019 25(3–4): p. 248–256. [PubMed: 30234441]
42. Moeinzadeh S, et al., Sequential Zonal Chondrogenic Differentiation of Mesenchymal Stem Cells in Cartilage Matrices. Tissue Engineering Part A, 2019 25(3–4): p. 234–247. [PubMed: 30146939]

43. Birchall JD and Chappell JS, The chemistry of aluminum and silicon in relation to Alzheimer's disease. Clin Chem, 1988 34(2): p. 265–7. [PubMed: 2830051]
44. Walakovits LA, et al., Detection of stromelysin and collagenase in synovial fluid from patients with rheumatoid arthritis and posttraumatic knee injury. Arthritis Rheum, 1992 35(1): p. 35–42. [PubMed: 1370619]
45. Yang X, et al., Effect of CD44 binding peptide conjugated to an engineered inert matrix on maintenance of breast cancer stem cells and tumorsphere formation. PLoS One, 2013 8(3): p. e59147. [PubMed: 23527117]
46. Moeinzadeh S, et al., Nanostructure Formation and Transition from Surface to Bulk Degradation in Polyethylene Glycol Gels Chain-Extended with Short Hydroxy Acid Segments. Biomacromolecules, 2013 14(8): p. 2917–2928. [PubMed: 23859006]
47. Keskar V, et al., In Vitro Evaluation of Macroporous Hydrogels to Facilitate Stem Cell Infiltration, Growth, and Mineralization. Tissue Engineering Part A, 2009 15(7): p. 1695–1707. [PubMed: 19119921]
48. Moeinzadeh S, Shariati SRP, and Jabbari E, Comparative effect of physicomechanical and biomolecular cues on zone-specific chondrogenic differentiation of mesenchymal stem cells. Biomaterials, 2016 92: p. 57–70. [PubMed: 27038568]
49. Guide For the Care and Use of Laboratory Animals, U.S. Department of Health and Human Services, Public Health Service, National Institutes of Health. 8th ed. 2011: National Academies Press.
50. Park KM, et al., Bone Regeneration Effect of Hyperbaric Oxygen Therapy Duration on Calvarial Defects in Irradiated Rats. Biomed Res Int, 2019 2019: p. 9051713. [PubMed: 31061829]
51. Zhang K, et al., Nanocomposite hydrogels stabilized by self-assembled multivalent bisphosphonate-magnesium nanoparticles mediate sustained release of magnesium ion and promote in-situ bone regeneration. Acta Biomater, 2017 64: p. 389–400. [PubMed: 28963020]
52. Lee JS, et al., Proof-of-concept study of vertical augmentation using block-type allogenic bone grafts: A preclinical experimental study on rabbit calvaria. J Biomed Mater Res B Appl Biomater, 2018 106(7): p. 2700–2707. [PubMed: 29411504]
53. Liu CN, et al., Nanoparticle contrast-enhanced micro-CT: A preclinical tool for the 3D imaging of liver and spleen in longitudinal mouse studies. J Pharmacol Toxicol Methods, 2019 96: p. 67–77. [PubMed: 30738209]
54. Abbasiliasi S, et al., Use of sodium alginate in the preparation of gelatin-based hard capsule shells and their evaluation in vitro. Rsc Advances, 2019 9(28): p. 16147–16157.
55. Seo BB, Koh JT, and Song SC, Tuning physical properties and BMP-2 release rates of injectable hydrogel systems for an optimal bone regeneration effect. Biomaterials, 2017 122: p. 91–104. [PubMed: 28110173]
56. Mahapatra C, Jin GZ, and Kim HW, Alginate-hyaluronic acid-collagen composite hydrogel favorable for the culture of chondrocytes and their phenotype maintenance. Tissue Engineering and Regenerative Medicine, 2016 13(5): p. 538–546. [PubMed: 30603434]
57. Pang XC, Lin LJ, and Tang B, Unraveling the role of Calcium ions in the mechanical properties of individual collagen fibrils. Scientific Reports, 2017 7.
58. Berg J, et al., Optimization of cell-laden bioinks for 3D bioprinting and efficient infection with influenza A virus. Scientific Reports, 2018 8.
59. Yang YL, Leone LM, and Kaufman LJ, Elastic moduli of collagen gels can be predicted from two-dimensional confocal microscopy. Biophys J, 2009 97(7): p. 2051–60. [PubMed: 19804737]
60. Odian G, Principles of Polymerization, 4th Edition. 2004: Wiley.
61. Nunamaker EA, Otto KJ, and Kipke DR, Investigation of the material properties of alginate for the development of hydrogel repair of dura mater. Journal of the Mechanical Behavior of Biomedical Materials, 2011 4(1): p. 16–33. [PubMed: 21094477]
62. Long C, et al., Isolation and characterization of canine placenta-derived mesenchymal stromal cells for the treatment of neurological disorders in dogs. Cytometry Part A, 2018 93a(1): p. 82–92.
63. Thomas D, et al., Temporal changes guided by mesenchymal stem cells on a 3D microgel platform enhance angiogenesis in vivo at a low-cell dose. Proc Natl Acad Sci U S A, 2020 117(32): p. 19033–19044. [PubMed: 32709748]

64. Cao N, Chen XB, and Schreyer DJ, Influence of Calcium Ions on Cell Survival and Proliferation in the Context of an Alginate Hydrogel. ISRN Chemical Engineering, 2012 2012: p. 516461.

65. Maia FR, et al., Effect of Cell Density on Mesenchymal Stem Cells Aggregation in RGD-Alginate 3D Matrices under Osteoinductive Conditions. Macromolecular Bioscience, 2014 14(6): p. 759–771. [PubMed: 24585449]

66. Markusen JF, et al., Behavior of adult human mesenchymal stem cells entrapped in alginate-GRGDY beads. Tissue Engineering, 2006 12(4): p. 821–830. [PubMed: 16674295]

67. Naito H, et al., The advantages of three-dimensional culture in a collagen hydrogel for stem cell differentiation. J Biomed Mater Res A, 2013 101(10): p. 2838–45. [PubMed: 23468218]

68. Nguyen BNB, et al., Collagen hydrogel scaffold promotes mesenchymal stem cell and endothelial cell coculture for bone tissue engineering. Journal of Biomedical Materials Research Part A, 2017 105(4): p. 1123–1131. [PubMed: 28093887]

69. Macdonald ML, et al., Tissue integration of growth factor-eluting layer-by-layer polyelectrolyte multilayer coated implants. Biomaterials, 2011 32(5): p. 1446–53. [PubMed: 21084117]

70. El Bialy I, Jiskoot W, and Reza Nejadnik M, Formulation, Delivery and Stability of Bone Morphogenetic Proteins for Effective Bone Regeneration. Pharm Res, 2017 34(6): p. 1152–1170. [PubMed: 28342056]

71. Medda L, Monduzzi M, and Salis A, The molecular motion of bovine serum albumin under physiological conditions is ion specific. Chem Commun (Camb), 2015 51(30): p. 6663–6. [PubMed: 25782536]

72. Mumcuoglu D, et al., Injectable BMP-2 delivery system based on collagen-derived microspheres and alginate induced bone formation in a time- and dose-dependent manner. Eur Cell Mater, 2018 35: p. 242–254. [PubMed: 29697853]

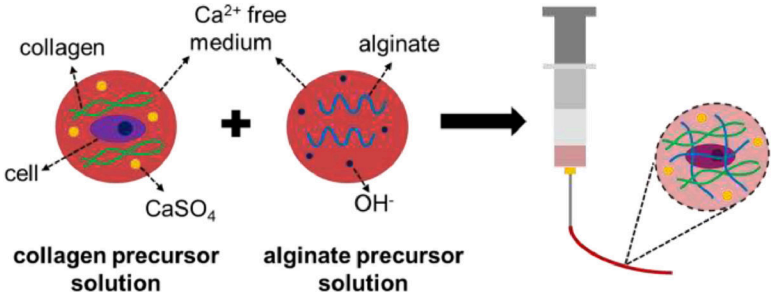

Figure 1.

Schematic diagram for injectable alg/col hydrogel preparation. The alginate precursor solution was prepared by dissolving alginate in calcium-free DMEM medium and adjusting the pH using NaOH. Collagen precursor solution was prepared by adding collagen to calcium-free DMEM medium and then supplementing the collagen solution with $CaSO_4$. hMSCs were suspended in collagen precursor solution and then two precursor solutions were pipette mixed.

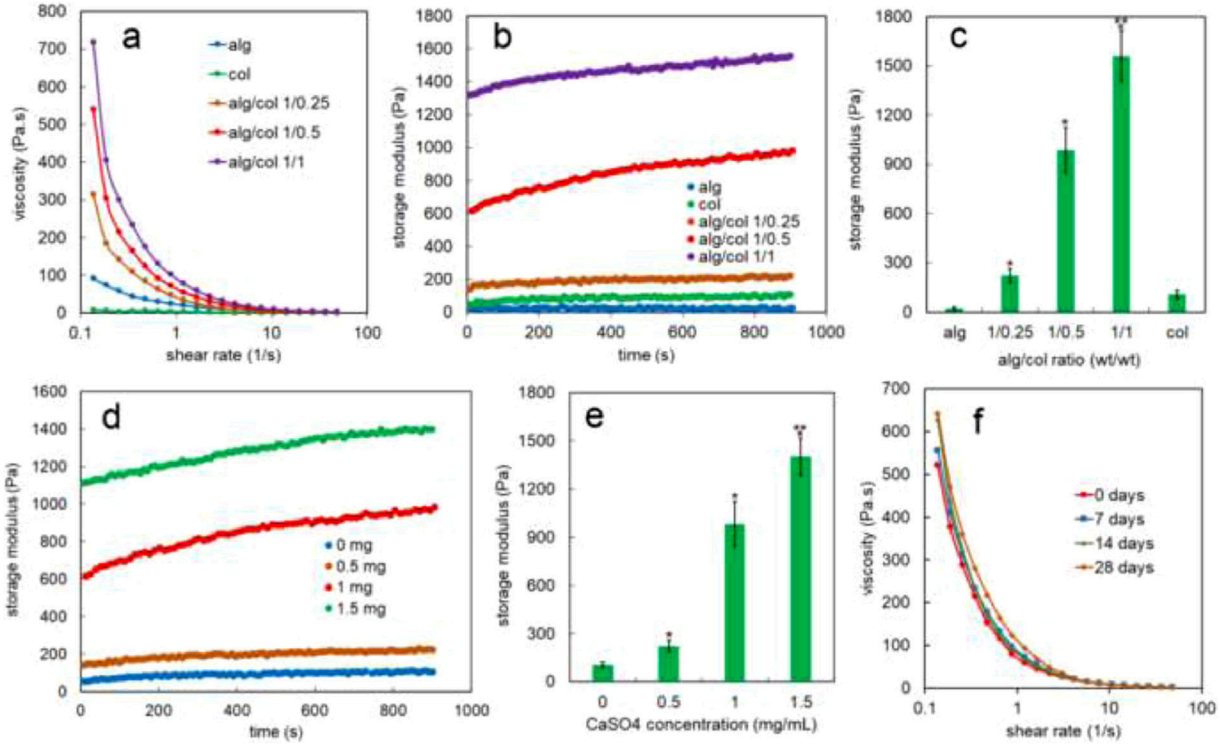

Figure 2.

(a) Effect of shear rate on the viscosity of alginate (alg, blue line), collagen (col, green line), alg/col 1/0.25 (brown line), alg/col 1/0.5 (red line), and alg/col 1/1 (purple line) hydrogels (b) evolution of storage modulus with time at 37 °C for alginate gel (blue), collagen (green), alg/col 1/0.25 (brown), alg/col 1/0.5 (red), and alg/col 1/1 (purple) hydrogels with 1 mg/mL $CaSO_4$ concentration (c) effect of alginate to collagen weight ratio on the storage modulus of alg/col gels after 900 seconds at 37 °C (d) evolution of storage modulus with time at 37 °C for alg/col 1/0.5 hydrogel with 0 (blue), 0.5 (brown), 1 (red), and 1.5 (green) mg/mL $CaSO_4$ concentration (e) effect of $CaSO_4$ concentration on the storage modulus of alg/col 1/0.5 hydrogel after 900 seconds at 37 °C. (f) effect of precursor solutions storage time on the shear dependent viscosity of the alg/col 1/0.5 hydrogel. The collagen and alginate precursor solutions were stored at 4°C for 0 days (red), 7 days (blue), 14 days (green), or 28 days (brown) and mixed right before the viscosity measurement. “An asterisk” in 2c represents a statistically significant difference between the test group and both alg and col groups. An asterisk in 2e represents a statistically significant difference between the test group and the group without $CaSO_4$. Two asterisks in 2c and 2e represents a statistically significant difference between the test group and all other groups. Error bars in 2c and 2e correspond to means ±1 SD for n = 3.

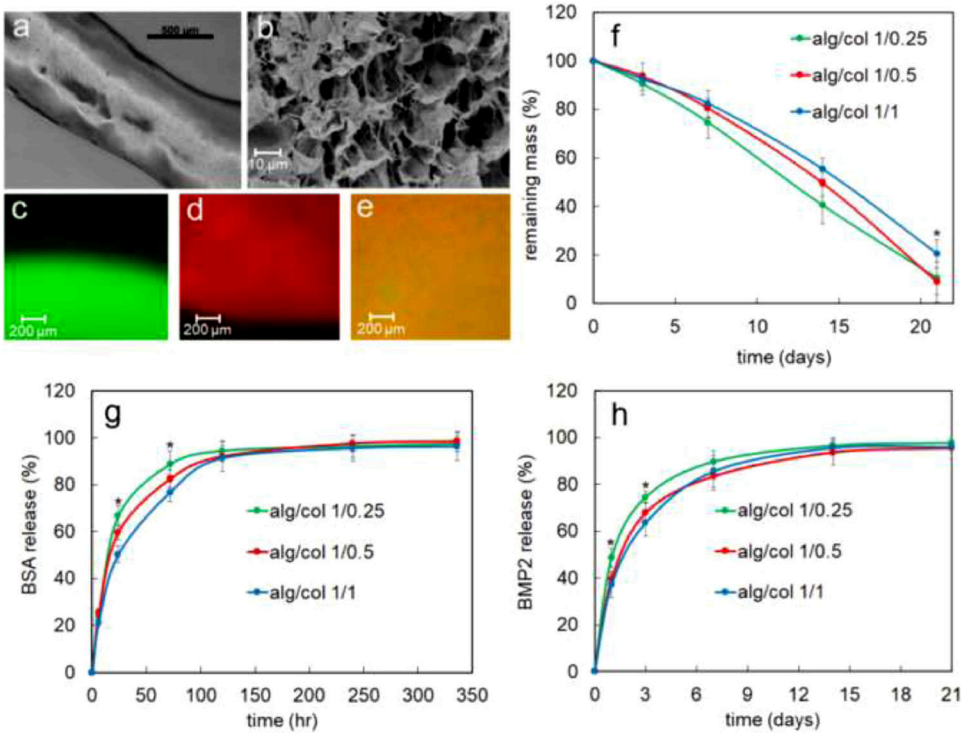

Figure 3.

(a) alg/col 1/0.5 gel strut injected from a 20G needle (b) A representative SEM image of alg/col 1/0.5 hydrogel (c) fluorescent image of alg/col alg (without collagen) prepared with green fluorescent-labeled alginate (d) fluorescent image of col hydrogel (without alginate) stained with red fluorescent dye (e) fluorescent image of alg/col 1/0.5 hydrogel that was prepared with green fluorescent-labeled alginate and then stained with red fluorescent dye to visualize collagen (f) degradation kinetics of alg/col 1/0.25 (green), alg/col 1/0.5 (red), and alg/col 1/1 (blue) hydrogels in PBS supplemented with collagenase and sodium citrate at 37°C. (g) release kinetics of BSA from alg/col 1/0.25 (green), alg/col 1/0.5 (red), and alg/col 1/1 (blue) hydrogels. (h) release kinetics of BMP2 from alg/col 1/0.25 (green), alg/col 1/0.5 (red), and alg/col 1/1 (blue) hydrogels. Error bars in 3f-3h correspond to means ±1 SD for n = 3. “An asterisk” in 3f, 3g, and 3h represents a statistically significant difference between the test group and all other groups at that time point.

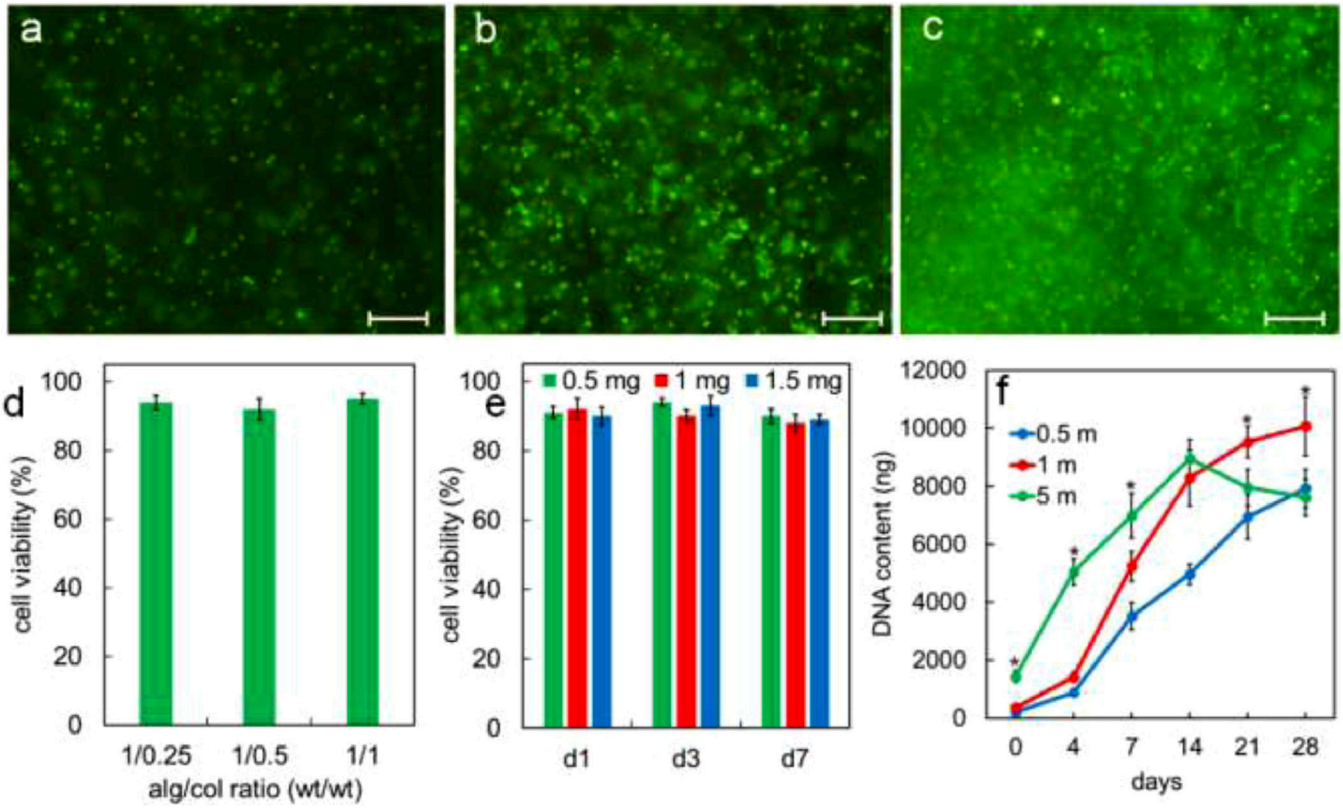

Figure 4.

live (green) and dead (orange) hMSCs encapsulated in alg/col 1/0.5 hydrogel with 0.5 million cells/mL (a), 1 million cells/mL (b) and 5 million cells/mL (c) cell densities 24hr after encapsulation. (d) effect of alginate to collagen weight ratio on the viability of hMSCs encapsulated in alg/col hydrogel with 1 million cells/mL density 24hr after encapsulation. (e) effect of $CaSO_4$ concentration in alg/col 1/0.5 hydrogels on the viability of encapsulated hMSCs (f) DNA content of hMSC-laden alg/col 1/0.5 hydrogels with cell densities of 0.5, 1 and 5 million cells/mL incubated in basal medium over 28 days. Scale bars in 4a-c are 100 μm. Error bars correspond to means ±1 SD for n = 3. “An asterisk” in 4f represents a significantly higher DNA content in the test group compared with all other groups at that time point.

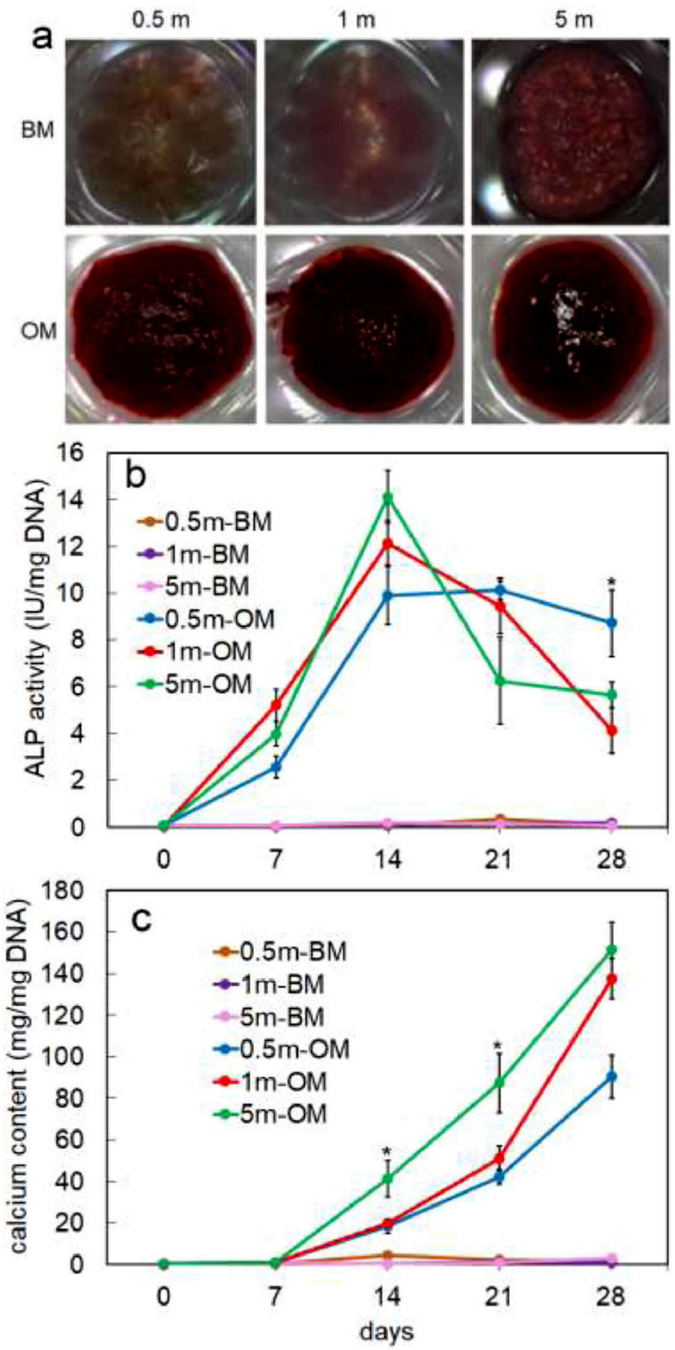

Figure 5.

(a) Alizarin red stained hMSC-laden alg/col 1/0.5 hydrogels with 0.5, 1 and 5 million cells/mL densities and incubated in basal medium (BM) or osteogenic medium (OM) for 28 days (b) ALP activity of hMSCs encapsulated in alg/col 1/0.5 hydrogels with 0.5, 1, or 5 million cells/mL density and incubated in BM or OM for 28 days (c) calcium content of hMSCs-laden alg/col 1/0.5 hydrogels with 0.5, 1, or 5 million cells/mL density and incubated in BM or OM for 28 days. “An asterisk” represents a statistically significant

difference between the test group and all other groups at that time point. Error bars correspond to means ±1 SD for n = 3.

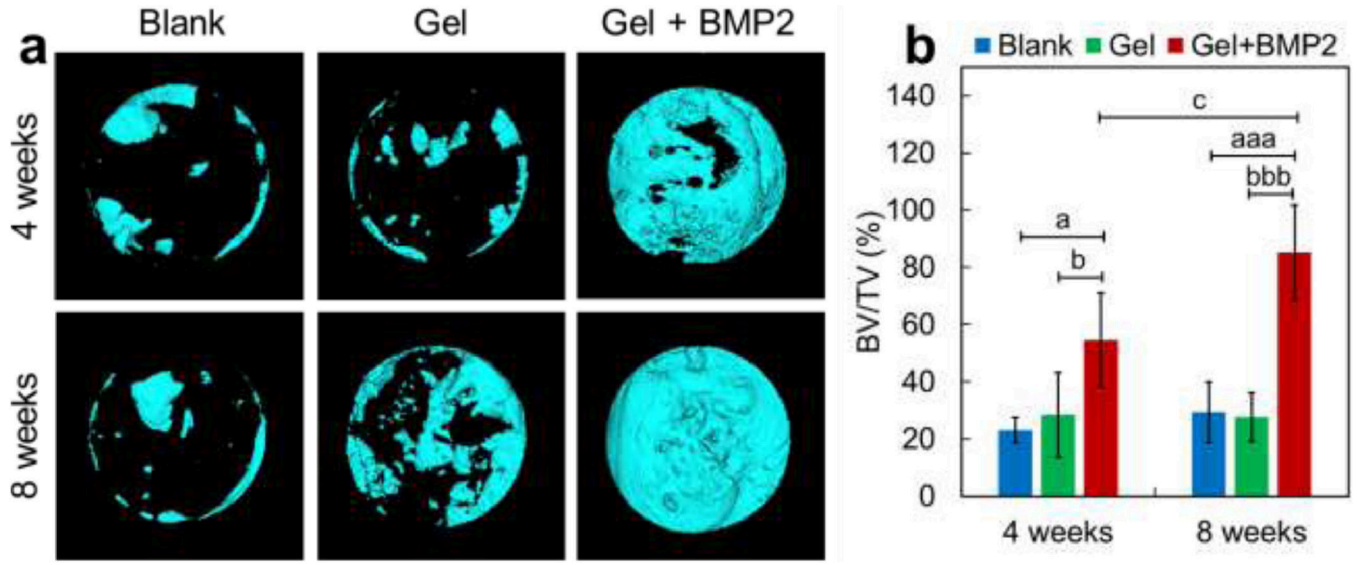

Figure 6.

(a,b) representative micro-CT reconstructed 3D images and the quantitative result of regenerated bone in the calvarial defect site. (a) 3D images of new bone formation in calvarial defect site without hydrogel injection (Blank) or with injection of alg/col 1/0.5 hydrogel alone (Gel) or BMP2-loaded alg/col 1/0.5 hydrogel (Gel + BMP2) after 4 weeks or 8 weeks. (b) Quantitative bone volume fraction (BV/TV) in calvarial defect site. Data are shown as mean ± SD (n = 6 per time point per group). $^{a}P < 0.05$, $^{aa}P < 0.01$, $^{aaa}P < 0.001$, vs. Blank group; $^{b}P < 0.05$, $^{bb}P < 0.01$, $^{bbb}P < 0.001$, vs. Gel group; $^{c}P < 0.05$, vs. Gel + BMP2 (4 weeks).

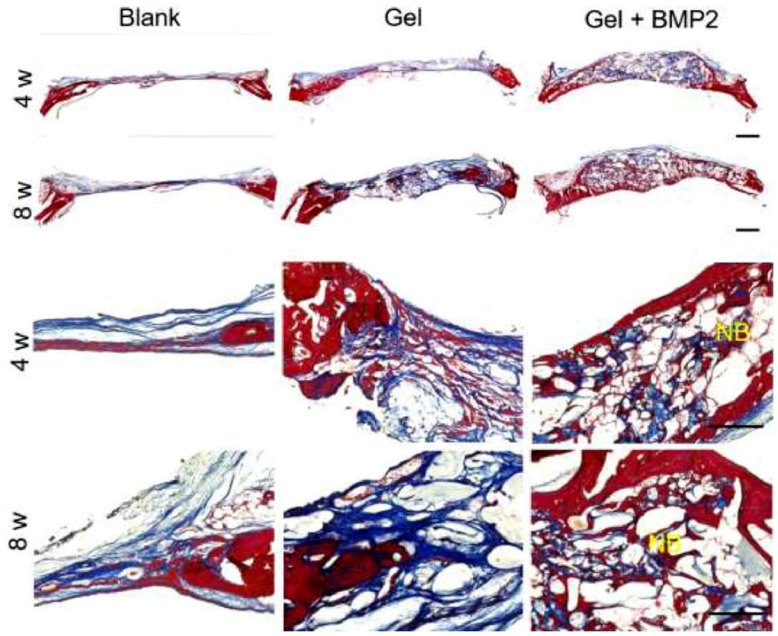

Figure 7.

Trichrome staining images of newly regenerated tissue in calvarial defect sites without hydrogel injection (Blank) or with injection of alg/col 1/0.5 hydrogel alone (Gel) or BMP2-loaded alg/col 1/0.5 hydrogel (Gel + BMP2) after 4 weeks or 8 weeks. Porous structure indicates hydrogel area. NB: new bone.

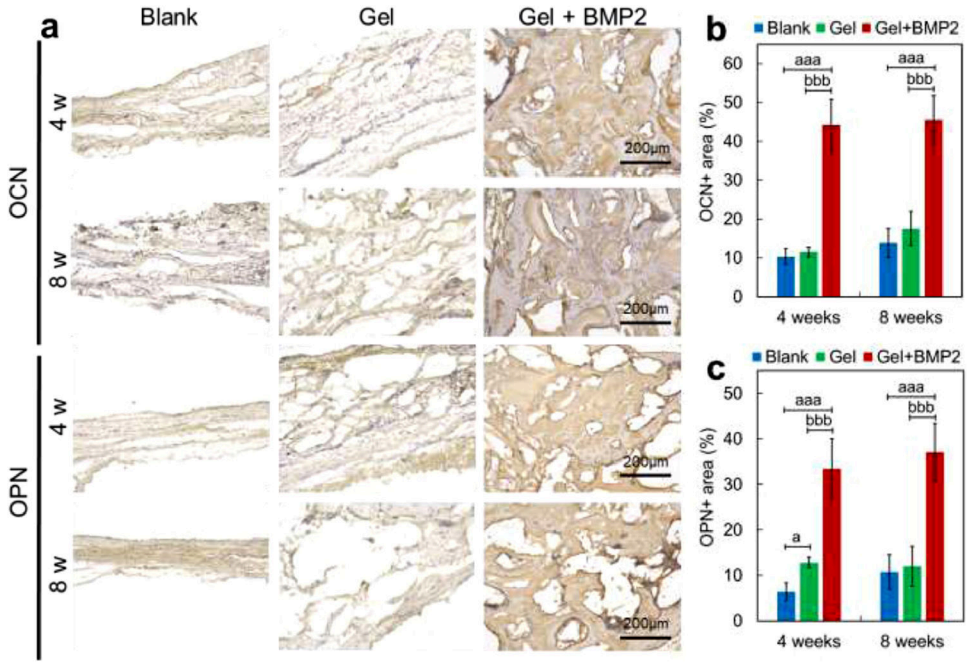

Figure 8.

results of immunohistochemical staining of osteocalcin (OCN) or osteopontin (OPN) at the newly regenerated tissue in calvarial defect site. (a) OCN and OPN staining images at the defect sites without hydrogel injection (Blank) or with injection of alg/col 1/0.5 hydrogel alone (Gel) or BMP2-loaded alg/col 1/0.5 hydrogel (Gel + BMP2) after 4 weeks or 8 weeks. (b, c) Quantitative percentages of OCN or OPN positive area in calvarial defect site. Data are shown as mean ± SD (n = 6 per time point per group). $^{a}P < 0.05$, $^{aa}P < 0.01$, $^{aaa}P < 0.001$, vs. Blank group; $^{b}P < 0.05$, $^{bb}P < 0.01$, $^{bbb}P < 0.001$, vs. Gel group.